© 2018. Published by The Company of Biologists Ltd | Journal of Cell Science (2018) 131, jcs211789. doi:10.1242/jcs.211789

RESEARCH ARTICLE

The phospholipase A_2 pathway controls a synaptic cholesterol ester cycle and synapse damage

Craig Osborne, Ewan West and Clive Bate*

ABSTRACT

The cellular prion protein (PrP^C) acts as a scaffold protein that organises signalling complexes. In synaptosomes, the aggregation of PrP^C by amyloid-β (Aβ) oligomers attracts and activates cytoplasmic phospholipase A_2 ($cPLA_2$), leading to synapse degeneration. The signalling platform is dependent on cholesterol released from cholesterol esters by cholesterol ester hydrolases (CEHs). The activation of $cPLA_2$ requires cholesterol released from cholesterol esters by cholesterol ester hydrolases (CEHs), enzymes dependent upon platelet activating factor (PAF) released by activated $cPLA_2$. This demonstrates a positive feedback system in which activated $cPLA_2$ increased cholesterol concentrations, which in turn facilitated $cPLA_2$ activation. PAF was also required for the incorporation of the tyrosine kinase Fyn and cyclooxygenase (COX)-2 into Aβ–PrP^C–$cPLA_2$ complexes. As a failure to deactivate signalling complexes can lead to pathology, the mechanisms involved in their dispersal were studied. PAF facilitated the incorporation of acyl-coenzyme A: cholesterol acyltransferase (ACAT)-1 into Aβ–PrP^C–$cPLA_2$–COX-2–Fyn complexes. The esterification of cholesterol reduced cholesterol concentrations, causing dispersal of Aβ–PrP^C–$cPLA_2$–COX-2–Fyn complexes and the cessation of signalling. This study identifies PAF as a key mediator regulating the cholesterol ester cycle, activation of $cPLA_2$ and COX-2 within synapses, and synapse damage.

KEY WORDS: Cholesterol, Esterification, Cyclooxygenase, Platelet-activating factor, Phospholipase A_2, Synaptosome

INTRODUCTION

The cellular prion protein (PrP^C) is mainly found in specific membrane micro-domains commonly called lipid rafts (Taraboulos et al., 1995). PrP^C acts as a scaffold protein that organises signalling complexes (Linden et al., 2012) and is associated with multiple signalling proteins, including the tyrosine kinase Fyn (Mouillet-Richard et al., 2000) and cytoplasmic phospholipase A_2 ($cPLA_2$) (Bate et al., 2010), which are linked to synapse degeneration. PrP^C is concentrated at synapses (Herms et al., 1999), and the aggregation of PrP^C (Chiesa et al., 2008) or cross-linkage of PrP^C with monoclonal antibodies (mAbs) (Solforosi et al., 2004) causes synaptic abnormalities. More recently, PrP^C has been identified as a receptor for amyloid-β (Aβ) oligomers (Laurén et al., 2009) which are responsible for the synapse degeneration and cognitive decline in patients with Alzheimer's disease (AD) (Selkoe, 2002; Shankar et al., 2008). The aggregation of PrP^C mediated by Aβ oligomers forms a signalling complex containing activated $cPLA_2$ and leads to synapse degeneration (Bate and Williams, 2011).

Cholesterol is a key component of lipid rafts (Brown and London, 2000) and, given that the formation and function of lipid rafts depends upon cholesterol concentrations (Rajendran and Simons, 2005), it follows that fluctuations in cholesterol concentrations may alter cell signalling within lipid rafts. We recently reported that soluble Aβ oligomers, highly toxic forms of Aβ (Yang et al., 2017), increased cholesterol concentrations in synaptosomes (West et al., 2017). This observation is consistent with reports showing that Aβ is concentrated in synapses (Lacor et al., 2004; Takahashi et al., 2010) and that the concentrations of cholesterol are increased in Aβ-positive synapses in the cortex of AD patients (Gylys et al., 2007). The increased cholesterol concentrations are dependent upon activated cholesterol ester hydrolases (CEHs) (West et al., 2017), which participate in the cholesterol ester cycle that controls membrane cholesterol concentrations (Chang et al., 2006). Thus, CEH inhibitors block both the Aβ-induced increase in cholesterol concentrations and Aβ-induced synapse damage in cultured neurons. However, the mechanisms leading to the activation of CEHs are poorly understood.

The present study investigated two key ideas. Firstly, we studied the signalling pathways leading to activation of CEHs in synaptosomes. The Aβ-induced activation of CEHs was dependent upon activation of $cPLA_2$ and the production of platelet-activating factor (PAF). The increased cholesterol concentrations stabilised a signalling platform containing Aβ, PrP^C, $cPLA_2$, Fyn and cyclooxygenase (COX)-2, and led to the production of prostaglandin E_2 (PGE_2). Concentrations of PGE_2 are raised in AD (Montine et al., 1999) and, in cultured neurons, PGE_2 causes extensive synapse damage (Bate et al., 2010).

In addition, this study examined the dissociation of signalling platforms as a physiological process that limits the intensity of signalling. Acyl-coenzyme A:cholesterol acyltransferase (ACAT)-1 was incorporated into Aβ–PrP^C–$cPLA_2$–COX-2–Fyn signalling complexes. The esterification of cholesterol by this enzyme reduced cholesterol concentrations, leading to the dissociation of complexes and reduced cell signalling. We hypothesise that the dissociation of signalling complexes is a physiological process that limits the intensity of cell activation. Consequently, conditions that prevent the dissociation of signalling complexes may lead to sustained activation, cell disruption and disease.

RESULTS

$cPLA_2$ inhibitors and PAF antagonists blocked the Aβ-induced increase in cholesterol concentrations

Aβ in the soluble fraction of extracts from AD brains (hereafter, soluble AD brain extracts) activates synaptic CEHs, resulting in increased cholesterol concentrations (West et al., 2017). The AD brain extracts used in the assays of the present study contained predominantly Aβ monomers, dimers and trimers, as shown by

Department of Pathology and Pathogen Biology, Royal Veterinary College, Hawkshead Lane, North Mymms, Hatfield, UK AL9 7TA.

*Author for correspondence (cbate@rvc.ac.uk)

C.B., 0000-0002-1378-0005

Received 4 October 2017; Accepted 19 March 2018

Journal of Cell Science (2018) 131, jcs211789. doi:10.1242/jcs.211789

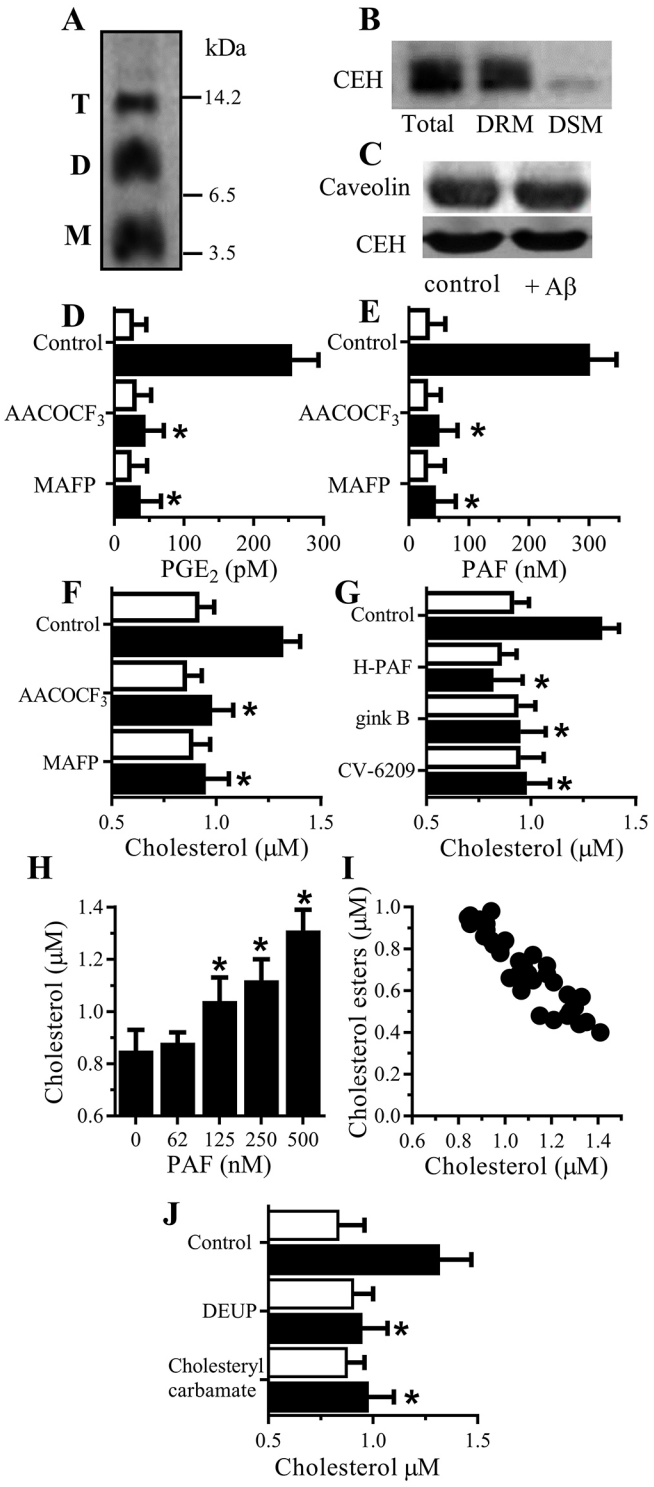

Fig. 1. PLA_2 inhibitors and PAF antagonists block the Aβ-induced increase in cholesterol concentrations. (A) Immunoblot showing forms of Aβ in soluble AD brain extract, including monomers (M), dimers (D) and trimers (T). (B) The amounts of CEHs in total cell membranes, DRMs and DSMs from synaptosomes. (C) The amounts of CEHs and caveolin in synaptosomes incubated with control medium or AD brain extract containing 1 nM $Aβ_{42}$. The concentrations of (D) PGE_2 and (E) PAF in synaptosomes pre-treated with a vehicle control or $cPLA_2$ inhibitors (1 μM $AACOCF_3$ or 1 μM MAFP) and incubated with either control medium (white bars) or AD brain extract containing 1 nM $Aβ_{42}$ (black bars). Values are means±s.d. from triplicate experiments performed three times; n=9. * indicate PGE_2/PAF concentrations significantly lower than those of synaptosomes incubated with AD brain extract. The concentrations of cholesterol in synaptosomes pre-treated with (F) a vehicle control or $cPLA_2$ inhibitors (1 μM $AACOCF_3$ or 1 μM MAFP), or (G) PAF antagonists [1 μM H-PAF, 1 μM ginkgolide B (gink B) or 1 μM CV-6209] as shown and incubated with control medium (white bars) or AD brain extract containing 1 nM $Aβ_{42}$ (black bars). Values are means±s.d. from triplicate experiments performed three times; n=9. * indicate cholesterol concentrations significantly lower than those of synaptosomes incubated with AD brain extract. (H) The cholesterol concentrations of synaptosomes incubated with PAF as shown. Values are means±s.d. from triplicate experiments performed three times; n=9. * indicate cholesterol concentrations significantly higher than those in control synaptosomes. (I) There was a significant inverse correlation between the concentrations of cholesterol and cholesterol esters in synaptosomes incubated with PAF (62 to 500 nM); Pearson's coefficient=−0.93, P<0.01. (J) The cholesterol concentrations of synaptosomes pre-treated with a vehicle control, DEUP, or cholesteryl N-(2-dimethylaminoethyl)carbamate and incubated with control medium (white bars) or 500 nM PAF (black bars). Values are means±s.d. from triplicate experiments performed three times; n=9.

immunoblotting (Fig. 1A). Initially, we looked at whether AD brain extracts affected the amounts and location of CEHs. CEHs in synaptosomes were found to be predominantly within detergent-resistant membranes (DRMs) (a crude measure of lipid rafts) (Fig. 1B). Synaptosomes incubated with soluble AD brain extract for 1 h did not have different amounts of CEHs (or caveolin, a loading control) compared with that in synaptosomes incubated with control medium (Fig. 1C). Because Aβ activates $cPLA_2$ (Palavicini et al., 2017; Zhu et al., 2006), we sought to determine whether activated $cPLA_2$ was involved in the increased synaptic cholesterol concentrations by using two selective $cPLA_2$ inhibitors [arachidonyl trifluoromethyl ketone ($AACOCF_3$) and methyl arachidonyl fluorophosphonate (MAFP)]. The activation of $cPLA_2$ is the first step in the production of bioactive lipids [including prostaglandins (PGs) and PAF] that affect synapse function (Clark et al., 1992; Sang et al., 2005). The addition of soluble AD brain extract to synaptosomes increases the production of PGE_2 in an Aβ-dependent manner (West et al., 2017). Here, we show that incubation with soluble AD brain extract also significantly increased concentrations of PAF in synaptosomes when compared with incubation with control medium (314±56 nM compared with 28±8 nM, n=6, P<0.01, mean±s.d.) or with Aβ-depleted soluble AD brain extract (314±56 nM compared with 32±10 nM, n=6, P<0.01). The Aβ-depleted soluble AD brain extract was prepared by incubation with mAb 4G8 (reactive with 17-24 of Aβ), which reduced the concentrations of $Aβ_{42}$ (1±0.07 nM $Aβ_{42}$ compared with 0.03±0.015 nM, n=9, P<0.01) and $Aβ_{40}$ (4.36±0.22 nM $Aβ_{40}$ compared with 0.24±0.07 nM, n=9, P<0.01) in AD brain extracts. In contrast, immunodepletion with mAb 3F4 (reactive with human prion proteins) had no significant effect on concentrations of $Aβ_{42}$ (1±0.07 nM $Aβ_{42}$ compared with 0.98±0.08 nM, n=9, P=0.38) and $Aβ_{40}$ (4.36±0.22 nM $Aβ_{40}$ compared with 4.15±0.28 nM, n=9, P=0.45). Pre-treatment of synaptosomes with 1 μM $AACOCF_3$ or 1 μM MAFP reduced the Aβ-induced increase in PGE_2 (Fig. 1D) and PAF (Fig. 1E), indicating that these concentrations of drugs inhibited $cPLA_2$.

Although there were no significant differences in cholesterol concentrations between synaptosomes treated with a vehicle control and those treated with 1 μM $AACOCF_3$ or with 1 μM MAFP, the Aβ-induced increase in cholesterol concentrations was reduced in synaptosomes pre-treated with 1 μM $AACOCF_3$ or with 1 μM MAFP (Fig. 1F). Next, the downstream products of $cPLA_2$ activation were examined in more detail. Pre-treatment of synaptosomes with inhibitors of COXs (5 μM acetyl salicylic acid or 5 μM ibuprofen), the enzymes that metabolise arachidonic acid to PGs, did not affect

Journal of Cell Science (2018) 131, jcs211789. doi:10.1242/jcs.211789

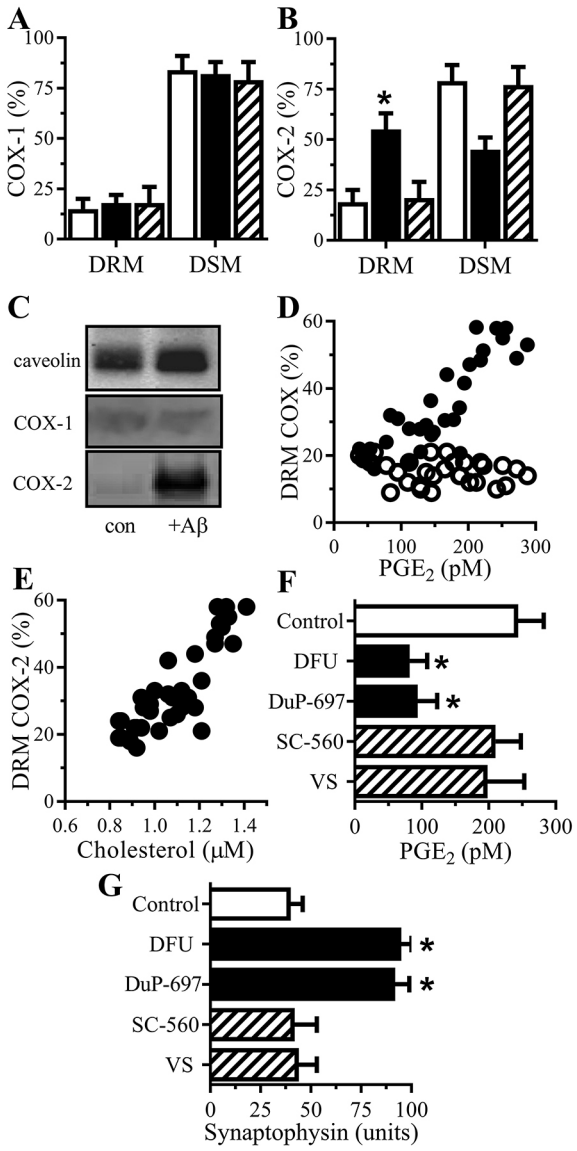

Fig. 2. Aβ caused the translocation of COX-2 into DRMs. The percentage of (A) COX-1 or (B) COX-2 in DRMs and DSMs derived from synaptosomes incubated with control medium (white bars), AD brain extract containing 1 nM $A\beta_{42}$ (black bars) or Aβ-depleted AD brain extract (striped bars). Values are means±s.d. from triplicate experiments performed three times; *n*=9. * indicates significantly more COX-2 in DRMs than in control synaptosomes. (C) Immunoblots showing the amounts of caveolin, COX-1 and COX-2 in DRMs from synaptosomes incubated with control medium or with AD brain extract containing 1 nM $A\beta_{42}$. (D) There was a significant correlation between the amounts of COX-2 (black circles), but not COX-1 (white circles), in DRMs and concentrations of PGE_2 in synaptosomes incubated with AD brain extract containing $A\beta_{42}$ (0.125 to 1 nM); Pearson's coefficient=0.85, $P<0.01$. (E) There was a significant correlation between cholesterol concentrations and the amounts of COX-2 in DRMs in synaptosomes incubated with AD brain extract containing $A\beta_{42}$ (0.125 to 1 nM); Pearson's coefficient=0.85, $P<0.01$. (F) The concentrations of PGE_2 produced by synaptosomes pre-treated with a vehicle control (white bars), COX-2 inhibitors (10 μM DFU or 10 μM DuP-697; black bars) or COX-1 inhibitors [10 μM valeryl salicylate (VS) or 1 μM SC-560; striped bars] and incubated with AD brain extract containing 1 nM $A\beta_{42}$. Values are means±s.d. from triplicate experiments performed three times; *n*=9. * indicate concentrations of PGE_2 significantly lower than those from control synaptosomes incubated with AD brain extract. (G) The amounts of synaptophysin in neurons pre-treated with a vehicle control (white bars), COX-2 inhibitors (10 μM DFU or 10 μM DuP-697; black bars) or COX-1 inhibitors [10 μM valeryl salicylate (VS) or 1 μM SC-560; striped bars] and incubated with AD brain extract containing 1 nM $A\beta_{42}$. Values are means±s.d. from triplicate experiments performed three times; *n*=9. * indicate concentrations of synaptophysin significantly higher than in control neurons incubated with AD brain extract.

the Aβ-induced increase in cholesterol concentrations (data not shown). In contrast, pre-treatment of synaptosomes with PAF antagonists [Hexa-PAF (H-PAF), ginkgolide B or CV-6209] reduced the Aβ-induced increase in cholesterol concentrations (Fig. 1G), suggesting that PAF was a key molecule regulating synaptic cholesterol concentrations. Further studies showed that PAF caused a dose-dependent increase in cholesterol concentrations (Fig. 1H). This was accompanied by reductions in cholesterol ester concentrations in PAF-treated synaptosomes, and there was a significant inverse correlation between the concentrations of cholesterol and cholesterol esters (Fig. 1I). Taken together, these results suggest that the Aβ-induced activation of $cPLA_2$ was a source of PAF that subsequently activated CEHs. This hypothesis was supported by the observation that the PAF-induced increase in cholesterol concentrations was blocked by selective CEH inhibitors [diethylumbelliferyl phosphate (DEUP) and cholesteryl N-(2-dimethylaminoethyl)carbamate; Fig. 1J].

Aβ caused the translocation of COX-2 to DRMs

Because PGE_2 causes synapse degeneration in cultured neurons (Bate et al., 2010), the effects of drugs that inhibit COXs, enzymes that convert arachidonic acid to PGs, were studied. There are two major COX isoforms, and in untreated synaptosomes both COX-1 and COX-2 were found to be predominantly within detergent-soluble membranes (DSMs). The addition of soluble AD brain extract, but not Aβ-depleted soluble AD brain extract, caused some COX-2 to migrate into DRMs (Fig. 2B,C). However, the addition had no effect on the amounts of COX-1 or caveolin in DRMs (Fig. 2A,C). There was a significant correlation between the amounts of COX-2 in DRMs and the concentrations of PGE_2 produced by synaptosomes in response to Aβ (Pearson's coefficient=0.85, $P<0.01$; Fig. 2D). This was consistent with the hypothesis that Aβ activates the COX-2 isoform. Cholesterol is a major factor in the formation of DRMs (Xu et al., 2001), and there was a significant correlation between cholesterol concentrations and the amounts of COX-2 in DRMs in synaptosomes incubated with Aβ (Pearson's coefficient=0.85, $P<0.01$; Fig. 2E). Pre-treatment of synaptosomes with DFU or DuP-697 (COX-2-selective inhibitors; Copeland et al., 1994; Riendeau et al., 1997), but not valeryl salicylate or SC-560 (COX-1-selective inhibitors; Bhattacharyya et al., 1995; Smith et al., 1998), reduced the Aβ-induced increase in PGE_2 (Fig. 2F). Soluble AD brain extracts cause the Aβ-dependent loss of synaptic proteins, including synapsin-1, vesicle-associated membrane protein-1, synaptophysin and cysteine string protein, from cultured neurons in a tissue culture model of synapse degeneration (West et al., 2017). Here, the addition of soluble AD brain extracts reduced the amounts of synaptophysin in a dose-dependent manner. Pre-treatment of neurons with COX-2-selective inhibitors (DFU or DuP-697), but not COX-1-selective inhibitors (valeryl salicylate or SC-560), protected neurons against the Aβ-induced loss of synaptophysin (Fig. 2G).

PAF antagonists and CEH inhibitors reduced the Aβ-induced translocation of COX-2 to DRMs

The above results suggested that PAF activated CEHs, and that the consequent increased cholesterol concentrations facilitated the translocation of COX-2 to DRMs, activation of COX-2 and

Journal of Cell Science (2018) 131, jcs211789. doi:10.1242/jcs.211789

the production of PGE_2. In accordance with this theory, pre-treatment of synaptosomes with PAF antagonists (H-PAF, ginkgolide B or CV-6209) significantly reduced the Aβ-induced translocation of COX-2 into DRMs (Fig. 3A) and PGE_2 production (Fig. 3B). Similarly, pre-treatment of synaptosomes with CEH inhibitors [DEUP or cholesteryl N-(2-dimethylaminoethyl)-carbamate] reduced the Aβ-induced translocation of COX-2 to DRMs (Fig. 3C) and PGE_2 production (Fig. 3D). The concentrations of PGE_2 produced by synaptosomes incubated with phospholipase A_2-activating peptide (PLAP, Bachem) were not significantly affected by pre-treatment with PAF antagonists (1 µM H-PAF or ginkgolide B) or CEH inhibitors [20 µM DEUP or 5 µM cholesteryl N-(2-dimethylaminoethyl)carbamate; Fig. 3E], indicating that these drugs did not affect $cPLA_2$ or COX-2 directly.

COX-2 is incorporated into Aβ–PrP^C complexes

We sought to determine whether COX-2 was associated with specific DRMs. PrP^C, a receptor that mediates Aβ toxicity (Laurén et al., 2009), acts as a scaffold protein and organises signalling complexes (Linden et al., 2012). The addition of soluble AD brain extract to synaptosomes caused the formation of Aβ–PrP^C complexes (Fig. 4A), and there was a significant correlation between the amounts of Aβ–PrP^C complexes and the amounts of COX-2 found within DRMs (Fig. 4B), suggesting a possible connection. Pre-treatment of synaptosomes with COX-2 inhibitors (DFU or DuP-697) did not affect the amounts of Aβ–PrP^C complexes formed (Fig. 4C), nor did they significantly alter the Aβ-induced increase in synaptic cholesterol concentrations (Fig. 4D). To isolate specific DRMs, synaptosomes incubated with soluble AD brain extract containing 1 nM $Aβ_{42}$ for 1 h were homogenised in a non-ionic detergent and incubated with the PrP^C-reactive mAb 4F2 (a gift from Professor J. Grassi, Paris, France). Immunoprecipitates containing PrP^C and associated DRM proteins were collected and analysed. These studies showed that CEHs did not co-precipitate with PrP^C. In contrast, $cPLA_2$, COX-2 and the tyrosine kinase Fyn all co-precipitated with PrP^C in synaptosomes incubated with soluble AD brain extract, but not in synaptosomes incubated with Aβ-depleted AD brain extract (Fig. 4E). Pre-treatment of synaptosomes with $AACOCF_3$ or H-PAF prevented the Aβ-induced incorporation of COX-2 and Fyn into PrP^C-containing DRMs (Fig. 4F). Similarly, pre-treatment of synaptosomes with CEH inhibitors reduced the Aβ-induced translocation of COX-2 and Fyn into DRMs (Fig. 4G). It is worth noting that the Aβ-induced translocation of $cPLA_2$ to DRMs (Bate and Williams, 2011) was not affected by either PAF antagonists or CEH inhibitors, nor did these drugs affect the amounts of caveolin in DRMs (Fig. 4G).

ACAT-1 is incorporated into Aβ–PrP^C complexes

The Aβ-induced changes in synaptic cholesterol concentrations are transient, and concentrations return to basal levels after 4 h, an effect mediated by ACAT-1 (West et al., 2017). The addition of soluble AD brain extract to synaptosomes caused ACAT-1 to translocate from DSMs to DRMs (Fig. 5A). The addition of Aβ-depleted AD brain extract did not significantly alter the amounts of ACAT-1 in DRMs. In addition, ACAT-1 co-precipitated with PrP^C-containing DRMs in synaptosomes incubated with soluble AD brain extract, but not in synaptosomes incubated with control medium or Aβ-depleted brain extract (Fig. 5B). Following the addition of soluble AD brain extract containing 0.6 to 1 nM $Aβ_{42}$ to synaptosomes, there were significant correlation between cholesterol concentrations and the amounts of ACAT-1 in DRMs (Fig. 5C), and between the amounts of Aβ–PrP^C complexes and ACAT-1 in DRMs (Fig. 5D). Pre-

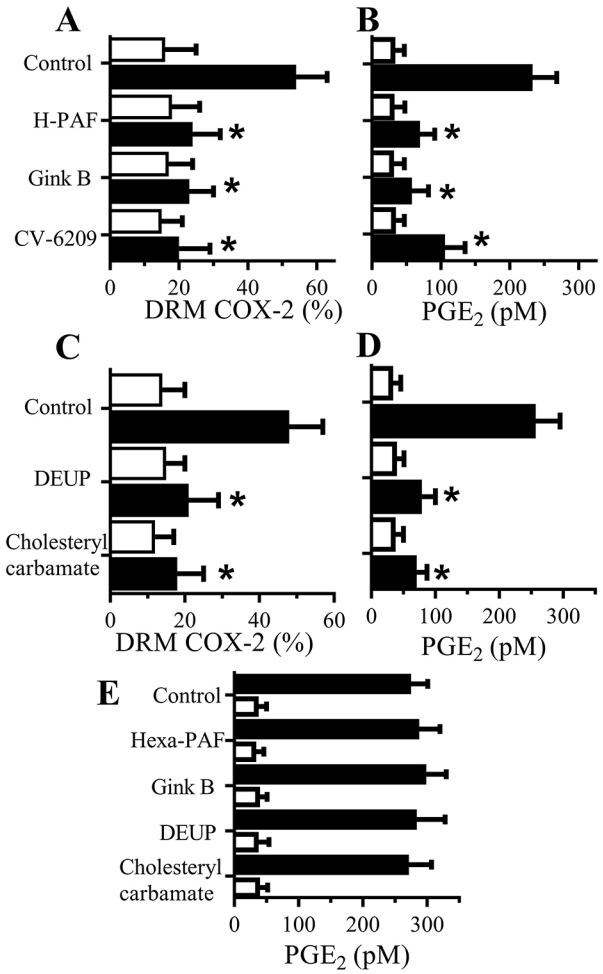

Fig. 3. PAF antagonists and CEH inhibitors reduced the Aβ-induced translocation of COX-2 into DRMs. The amounts of (A) COX-2 in DRMs and (B) PGE_2 in synaptosomes pre-treated with a vehicle control or PAF antagonists (1 µM H-PAF, ginkgolide B or CV6209) and incubated with control medium (white bars) or AD brain extract containing 1 nM $Aβ_{42}$ (black bars). Values are means±s.d. from triplicate experiments performed three times; *n*=9. * indicate significantly less COX-2 in DRMs or PGE_2 than in control synaptosomes incubated with AD brain extract. The amounts of (C) COX-2 in DRMs and (D) PGE_2 in synaptosomes pre-treated with a vehicle control or CEH inhibitors [20 µM DEUP or 5 µM cholesteryl N-(2-dimethylaminoethyl)-carbamate] and incubated with control medium (white bars) or AD brain extract containing 1 nM $Aβ_{42}$ (black bars). Values are means±s.d. from triplicate experiments performed three times; *n*=9. * indicate significantly less COX-2 in DRMs/PGE_2 than in control synaptosomes incubated with AD brain extract. (E) The concentrations of PGE_2 in synaptosomes pre-treated with a vehicle control, PAF antagonists (1 µM H-PAF or 1 µM ginkgolide B) or CEH inhibitors [20 µM DEUP or 5 µM cholesteryl N-(2-dimethylaminoethyl)carbamate] and incubated with control medium (white bars) or 500 nM PLAP (black bars). Values are means±s.d. from triplicate experiments performed three times; *n*=9.

treatment of synaptosomes with a $cPLA_2$ inhibitor ($AACOCF_3$), a PAF antagonist (H-PAF) or a CEH inhibitor (DEUP) reduced the Aβ-induced recruitment of ACAT-1 into DRMs (Fig. 5E,F). None of these treatments affected the amounts of caveolin found within DRMs (Fig. 5F).

Time-course studies showed that Aβ–PrP^C complexes (Fig. 6A) and the Aβ-induced targeting of COX-2 (Fig. 6B) and ACAT-1 (Fig. 6C) to DRMs were also transient in synaptosomes. The return of cholesterol concentrations to those of control synaptosomes is blocked by ACAT inhibitors (West et al.,

Journal of Cell Science (2018) 131, jcs211789. doi:10.1242/jcs.211789

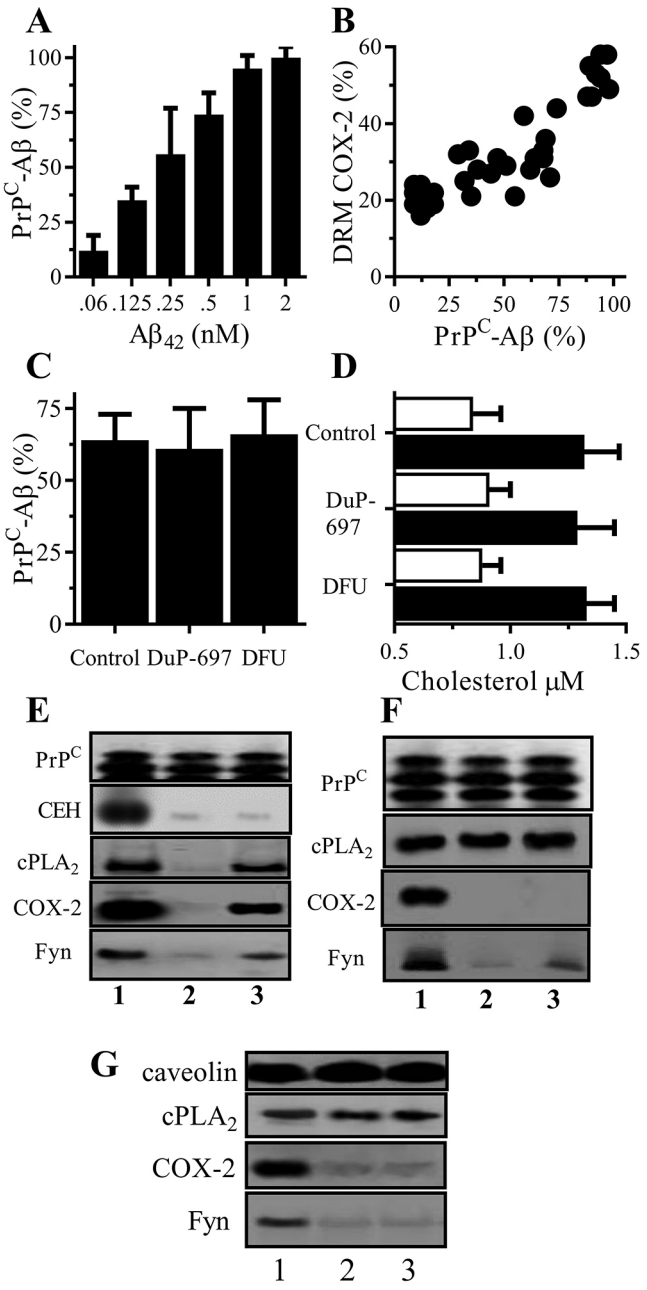

Fig. 4. CEH inhibitors blocked the Aβ-induced translocation of COX-2 to DRMs. (A) The amounts of Aβ–PrP^C complexes in synaptosomes incubated with AD brain extract containing $Aβ_{42}$ as shown. Values are means±s.d. from triplicate experiments performed three times; *n*=9. (B) There was a significant correlation between the amounts of Aβ–PrP^C complexes and the amounts of COX-2 in DRMs following the addition of AD brain extract containing $Aβ_{42}$ (0.06 to 1 nM), Pearson's coefficient=0.88, $P<0.01$. (C) The amounts of Aβ–PrP^C complexes in synaptosomes pre-treated with a vehicle control or COX-2 inhibitors (10 μM DFU or 10 μM DuP-697) and incubated with soluble AD brain extract containing 0.5 nM $Aβ_{42}$. Values are means±s.d. from triplicate experiments performed three times; *n*=9. (D) The cholesterol concentrations in synaptosomes pre-treated with a vehicle control or COX-2 inhibitors (10 μM DFU or 10 μM DuP-697) and incubated with control medium (white bars) or with soluble AD brain extract containing 0.5 nM $Aβ_{42}$ (black bars). Values are means±s.d. from triplicate experiments performed three times; *n*=9. (E) The amounts of PrP^C, CEH, $cPLA_2$, COX-2 and Fyn in (1) synaptosomes or co-precipitated with PrP^C from synaptosomes incubated with (2) Aβ-depleted AD brain extract or (3) AD brain extract containing 1 nM $Aβ_{42}$. (F) The amounts of PrP^C, $cPLA_2$, COX-2 and Fyn co-precipitated with PrP^C from synaptosomes pre-treated with (1) a vehicle control, (2) a $cPLA_2$ inhibitor (1 μM AACOCF$_3$) or (3) a PAF antagonist (1 μM H-PAF) and incubated with AD brain extract containing 1 nM $Aβ_{42}$. (G) Immunoblot showing the amounts of caveolin, $cPLA_2$, COX-2 and Fyn in DRMs from synaptosomes pre-treated with (1) a vehicle control or CEH inhibitors (2) 20 μM DEUP or (3) 5 μM cholesteryl N-(2-dimethylaminoethyl)carbamate and incubated with AD brain extract containing 1 nM $Aβ_{42}$.

2017). Here, we demonstrate that pre-treatment of synaptosomes with ACAT inhibitors (TMP-153 or YIC-C8-434) significantly increased the longevity of Aβ–PrP^C complexes. Pre-treatment with ACAT inhibitors also increased the amounts of COX-2 and ACAT-1 in DRMs at 2 and 4 h after the addition of Aβ (Fig. 6B,C), indicating that cholesterol esterification mediates the disruption of signalling complexes. This hypothesis was supported by the observation that pre-treatment with ACAT inhibitors also increased the Aβ-induced production of PGE_2 (Fig. 6D) and significantly increases synapse damage in neurons incubated with Aβ (West et al., 2017).

Cytochalasin D blocked the Aβ-induced translocation of COX-2 and ACAT-1 into DRMs

Because PrP^C signalling is dependent upon endocytosis (Caetano et al., 2008), the effects cytochalasin D (100 nM), which inhibits endocytosis into the recycling pathway (Millman et al., 2008), on Aβ–PrP^C complexes was studied. There were significantly higher amounts of Aβ–PrP^C complexes at the surface of synaptosomes (released by the membrane-impermeable enzyme phosphatidylinositol-phospholipase C) pre-treated with cytochalasin D and incubated with soluble AD brain extract containing 1 nM $Aβ_{42}$ than in synaptosomes pre-treated with a vehicle control (Fig. 7A), showing that cytochalasin D inhibited the endocytosis of Aβ–PrP^C complexes. In addition, pre-treatment with cytochalasin D prevented the dissociation of Aβ–PrP^C complexes (Fig. 7B). In cytochalasin D-treated synaptosomes incubated with soluble AD brain extract, both the cholesterol concentrations (Fig. 7C) and the amount of $cPLA_2$ within DRMs (Fig. 7D) remained higher than those in synaptosomes pre-treated with a vehicle control. In contrast, pre-treatment of synaptosomes with cytochalasin D reduced the Aβ-induced translocation of COX-2 (Fig. 7E) and ACAT-1 (Fig. 7F) into DRMs, suggesting that these events occur within an intracellular compartment. Co-immunoprecipitation studies with the PrP^C-reactive mAb 4F2 showed that cytochalasin D reduced the Aβ-induced translocation of COX-2 and ACAT-1 to Aβ–PrP^C complexes, but did not affect the translocation of $cPLA_2$ or Fyn (Fig. 7G). Cytochalasin D also reduced the Aβ-induced PGE_2 production from 265±39 pM PGE_2 to 91±19 pM PGE_2 (*n*=6, $P<0.01$). These results suggest that Aβ bound to PrP^C forms a functional signalling complex only in an intracellular compartment. Finally, we report that pre-treatment of cultured neurons with 100 nM cytochalasin D reduced the Aβ-induced loss of synaptophysin (Fig. 7H).

DISCUSSION

Although CEHs are key enzymes involved in the formation of Aβ-induced signalling complexes (West et al., 2017), little is known about how they are activated. Here, we show that $cPLA_2$ and PAF are key intermediates in the Aβ-induced activation of CEHs in synaptosomes and that they increase cholesterol concentrations. The increase in cholesterol concentrations facilitates the formation of signalling complexes, leading to synapse degeneration in neurons (Bate et al., 2010).

Journal of Cell Science (2018) 131, jcs211789. doi:10.1242/jcs.211789

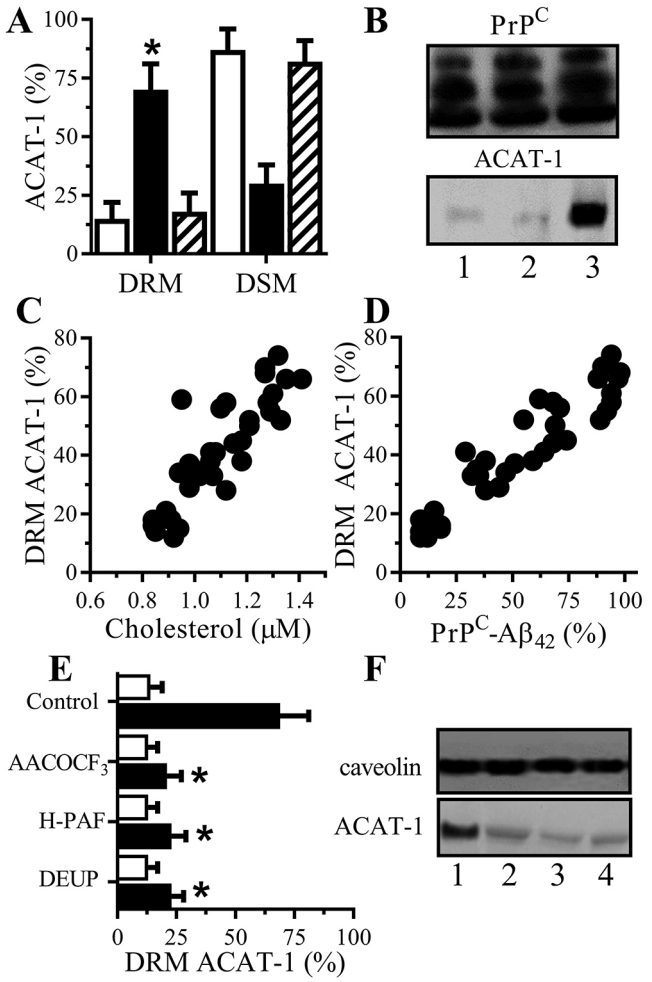

Fig. 5. Aβ caused the translocation of ACAT-1 to PrP^C complexes. (A) The amounts of ACAT-1 in DRMs and DSMs from synaptosomes incubated with control medium (white bars), AD brain extract containing 1 nM Aβ_{42} (black bars) or Aβ-depleted AD brain extract (striped bars). Values are means±s.d. from triplicate experiments performed three times; *n*=9. * indicates significantly more ACAT-1 than in control synaptosomes. (B) Immunoblots showing the amounts of ACAT-1 co-precipitated with PrP^C from synaptosomes incubated with (1) control medium, (2) Aβ-depleted AD brain extract or (3) AD brain extract containing 1 nM Aβ_{42}. There were significant correlations between (C) the amounts of ACAT-1 in DRMs and cholesterol concentrations; Pearson's coefficient=0.82, *P*<0.01, and (D) the amounts of ACAT-1 in DRMs and Aβ–PrP^C complexes; Pearson's coefficient=0.94, *P*<0.01, following the addition of AD brain extract containing Aβ_{42} (0.06 to 1 nM) to synaptosomes. (E) The amounts of ACAT-1 in DRMs from synaptosomes pre-treated with a vehicle control, 1 μM AACOCF$_3$, 1 μM H-PAF or 20 μM DEUP and incubated with control medium (white bars) or AD brain extract containing 1 nM Aβ_{42} (black bars). * indicate significantly less ACAT-1 than in control synaptosomes incubated with AD brain extract. (F) Immunoblots showing the amounts of caveolin and ACAT-1 in DRMs from synaptosomes pre-treated with (1) a vehicle control, (2) 1 μM AACOCF$_3$, (3) 1 μM H-PAF or (4) 20 μM DEUP and incubated with AD brain extract containing 1 nM Aβ_{42}.

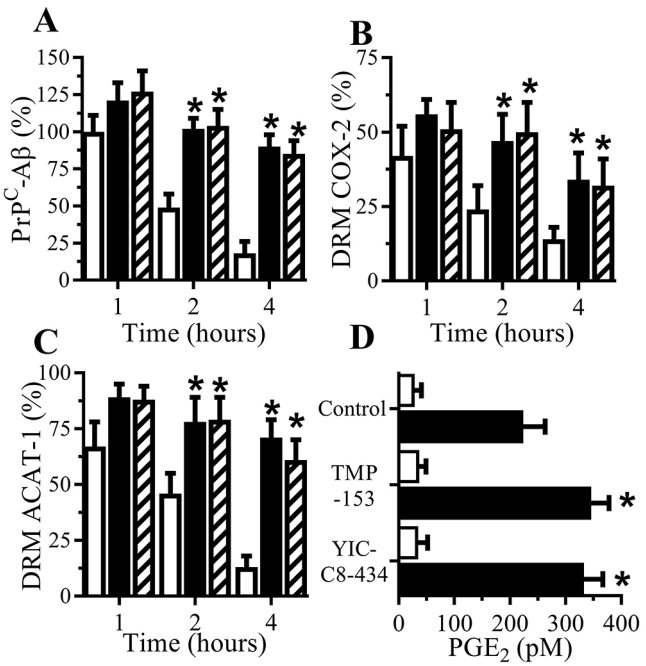

Fig. 6. Cholesterol esterification dispersed Aβ–PrP^C complexes. (A) The amounts of Aβ–PrP^C complexes in synaptosomes pre-treated with a vehicle control (white bars) or ACAT inhibitors (TMP-153, black bars or YIC-C8-434, striped bars) and incubated with AD brain extract containing 1 nM Aβ_{42} for time periods as shown. Values are means±s.d. from triplicate experiments performed three times; *n*=9. * indicate amounts of Aβ–PrP^C complexes significantly higher than in untreated synaptosomes incubated with AD brain extract. The amounts of (B) COX-2 and (C) ACAT-1 within DRMs in synaptosomes pre-treated with a vehicle control (white bars) or ACAT inhibitors (TMP-153, black bars or YIC-C8-434, striped bars) and incubated with AD brain extract containing 1 nM Aβ_{42} for time periods as shown. Values are means±s.d. from triplicate experiments performed three times; *n*=9. * indicate amounts of COX-2 or ACAT-1 significantly higher than in control synaptosomes incubated with AD brain extract. (D) The concentrations of PGE$_2$ produced by synaptosomes pre-treated with a vehicle control, 100 nM TMP-153 or 100 nM YIC-C8-434 and incubated with control medium (white bars) or with AD brain extract containing 1 nM Aβ_{42} (black bars). * indicate concentrations of PGE$_2$ significantly higher than control synaptosomes incubated with AD brain extract.

Activation of cPLA$_2$ was a key step in the Aβ-induced increase in synaptic cholesterol concentrations. Although activated cPLA$_2$ can give rise to multiple biologically active lipids, including lyso-phospholipids, our studies were concentrated on the effects of PAF for two reasons. Firstly, because PAF antagonists blocked the Aβ-induced increase in synaptic cholesterol concentrations and, secondly, because PAF also increased synaptic cholesterol concentrations via activation of CEHs. The movement of enzymes to and from membranes containing substrates is a key mechanism of cell regulation. The increase in cholesterol concentrations facilitated the movement of key signalling enzymes, COX-2 and Fyn into DRMs. These results support the hypothesis that Aβ activates the COX-2 isoform. Selective COX-2 inhibitors did not affect the formation of Aβ–PrP^C complexes or the Aβ-induced increase in synaptic cholesterol concentrations. However, COX-2-selective inhibitors reduced the Aβ-induced increase in PGE$_2$ concentrations and protected neurons against Aβ-induced synapse damage. These results are consistent with reports showing that COX-2 is expressed at the synapse (Kaufmann et al., 1996) and that COX-2 inhibitors reverse Aβ-mediated suppression of long-term potentiation and memory (Kotilinek et al., 2008).

In synaptosomes incubated with Aβ, COX-2 co-precipitated with PrP^C, cPLA$_2$ and Fyn, suggesting that it formed part of a signalling complex. The Aβ-induced translocation of COX-2 and Fyn to Aβ–PrP^C complexes and the production of PGE$_2$ were dependent upon the PAF-induced increase in cholesterol concentrations. PAF antagonists and CEH inhibitors did not affect all DRM proteins; for example, they did not affect the amounts of caveolin in DRMs, nor did they affect the Aβ-induced translocation of cPLA$_2$ to DRMs.

Journal of Cell Science (2018) 131, jcs211789. doi:10.1242/jcs.211789

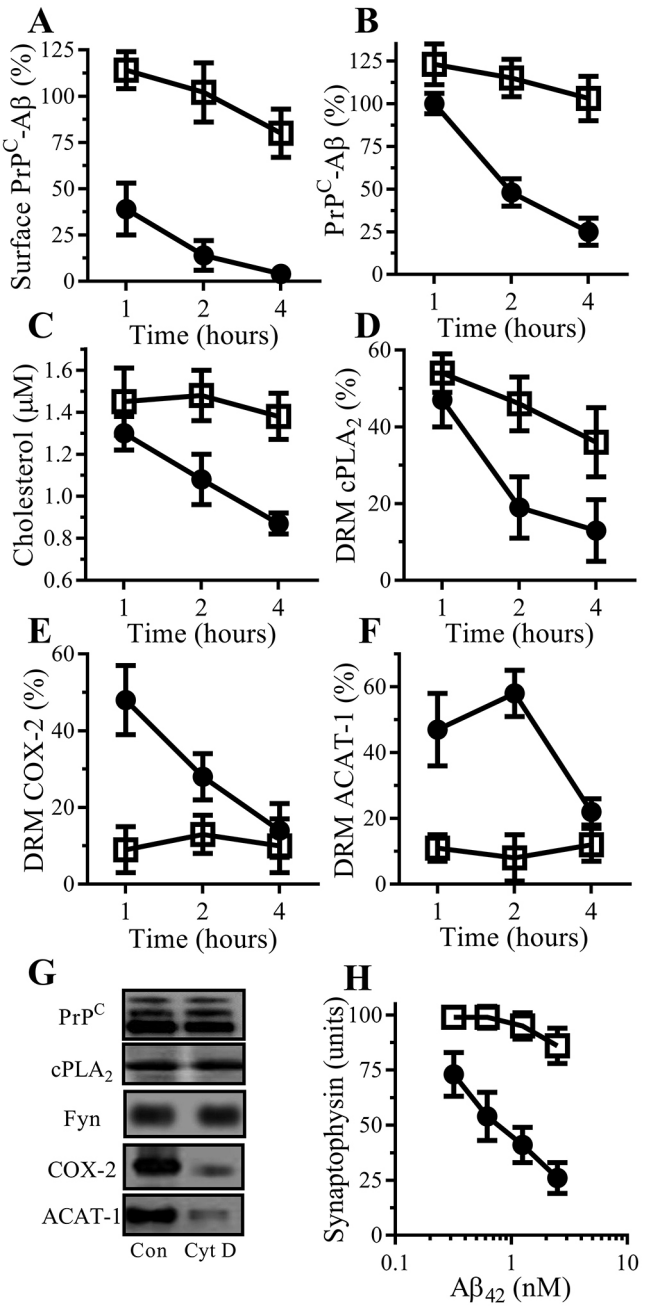

Fig. 7. Cytochalasin D blocked the Aβ-induced translocation of COX-2 and ACAT-1 into signalling complexes. (A) The amounts of Aβ–PrP^C complexes at the surface of synaptosomes, and (B) total amounts of Aβ–PrP^C complexes in synaptosomes after pre-treatment with a vehicle control (black circles) or 100 nM cytochalasin D (white squares) and incubation with AD brain extract containing 1 nM $Aβ_{42}$. Values are means±s.d. from triplicate experiments performed three times; *n*=9. (C) The concentrations of cholesterol and the amounts of (D) $cPLA_2$, (E) COX-2 and (F) ACAT-1 in DRMs from synaptosomes pre-treated with a vehicle control (black circles) or 100 nM cytochalasin D (white squares) and incubated with AD brain extract containing 1 nM $Aβ_{42}$. Values are means±s.d. from triplicate experiments performed three times; *n*=9. (G) The amounts of PrP^C, $cPLA_2$, Fyn, COX-2 and ACAT-1 in DRMs precipitated by the anti-PrP^C mAb 4F2 in synaptosomes pre-treated with a vehicle control or 100 nM cytochalasin D and incubated with AD brain extract containing 1 nM $Aβ_{42}$. (H) The amounts of synaptophysin in neuronal cultures pre-treated with a vehicle control (black circles) or 100 nM cytochalasin D (white squares) and incubated with AD brain extract containing $Aβ_{42}$ as shown. Values are means±s.d. from triplicate experiments performed three times; *n*=9.

Furthermore, neither PAF antagonists nor CEH inhibitors affected the production of PGE_2 by synaptosomes incubated with PLAP, indicating that they do not affect $cPLA_2$ or COX-2 directly. These observations are consistent with the hypothesis that PAF antagonists and CEH inhibitors modify the membrane environment generated by Aβ that leads to PGE_2 production.

Aβ is produced as part of normal neuronal metabolism (Haass et al., 1992), and plays a role in regular synapse function and memory formation (Abramov et al., 2009; Garcia-Osta and Alberini, 2009; Puzzo et al., 2011). The observations that PAF and PGE_2 affect synapse function and memory formation at physiological concentrations (Chen and Bazan, 2005; Chen et al., 2001; Clark et al., 1992; Kato et al., 1994; Koch et al., 2010) are consistent with the theory that Aβ-induced activation of $cPLA_2$ and the production of PAF and PGE_2 are part of normal synapse function. The observations that concentrations of PAF (Ryan et al., 2009) and PGE_2 (Montine et al., 1999) are elevated in the brains of AD patients indicate that this pathway is activated in the brains of AD patients. Reports showing that PAF and PGE_2 cause synapse damage in cultured neurons (Bate et al., 2010) suggest that aberrant activation of this pathway causes synapse degeneration. Consequently, it is crucial to understand how this pathway is controlled.

The Aβ-induced translocation of ACAT-1 into DRMs, and more specifically Aβ–PrP^C complexes, was dependent upon PAF and CEH. Aβ–PrP^C complexes in synaptosomes were transient, and there was a close temporal association between cholesterol concentrations and Aβ–PrP^C complexes (West et al., 2017). Notably, pre-treatment of neurons with ACAT inhibitors significantly enhanced Aβ-induced synapse damage (West et al., 2017). Here, we show that pharmacological inhibition of ACAT reduced the dissociation of Aβ–PrP^C complexes, increasing the time COX-2 and ACAT-1 were found in DRMs and significantly increased the Aβ-induced production of PGE_2. ACAT inhibitors have been proposed as AD treatments as they reduce the production of Aβ, and ablation of ACAT-1 reduces pathology in transgenic AD mice (Bryleva et al., 2010; Puglielli et al., 2001). However, in these studies, ACAT was inhibited, or ablated, before pathology developed. Consequently, ACAT inhibitors might be able to prevent the development of AD pathology but may be contraindicated in the latter stages of AD, where concentrations of Aβ are already raised.

Although inhibition of endocytosis by means of cytochalasin D significantly reduced the Aβ-induced production of PGE_2, it had diverse effects upon the Aβ-induced signalling complex. Cytochalasin D disrupted the relationships between Aβ–PrP^C complexes, cholesterol concentrations and enzymes involved in PGE_2 production. Firstly, cytochalasin D maintained the Aβ-induced increase in cholesterol concentrations, stabilised Aβ–PrP^C complexes and increased the time $cPLA_2$ spent in DRMs. Although these changes might be expected to increase PGE_2 production, cytochalasin D also prevented the Aβ-induced translocation of COX-2 to DRMs/Aβ–PrP^C complexes. In addition, cytochalasin D reduced the Aβ-induced translocation of ACAT-1 to DRMs and Aβ–PrP^C complexes. The lack of ACAT-1 in DRMs explains the maintenance of high cholesterol concentrations and, consequently, the longevity of complexes in synaptosomes.

Collectively, these results suggest that Aβ causes a tri-phasic response. Firstly, aggregation of cell surface PrP^C by Aβ oligomers led to the translocation of $cPLA_2$ into DRMs, the activation of $cPLA_2$ and the release of PAF (Fig. 8A). PAF activated CEHs, resulting in the increased cholesterol concentrations that stabilised

Journal of Cell Science (2018) 131, jcs211789. doi:10.1242/jcs.211789

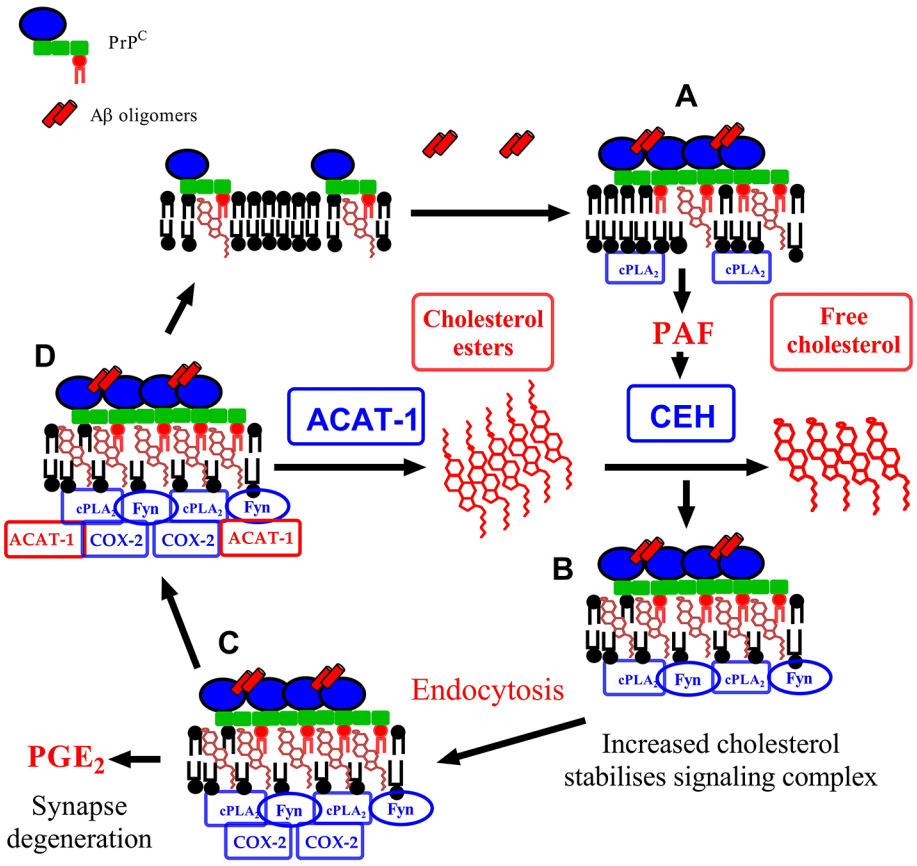

Fig. 8. Putative control of synaptic signalosome created by Aβ oligomers. (A) The binding of Aβ oligomers links PrP^C within lipid rafts; this recruits and activates $cPLA_2$ leading to the production of PAF. (B) PAF activates CEHs, causing the release of cholesterol into the membrane. The increase in cholesterol stabilises signalling complexes and recruits the tyrosine kinase Fyn. (C) Following endocytosis, COX-2 is recruited into the complex, leading to the release of PGE_2. High concentrations of PGE_2 cause synapse degeneration. (D) Recruitment of ACAT-1 into the complex results in the esterification of cholesterol, reduced cholesterol concentrations and the dispersal of lipid raft signalling complexes.

Aβ–PrP^C–$cPLA_2$ complexes and recruited Fyn (Fig. 8B). Secondly, endocytosis of Aβ–PrP^C–$cPLA_2$–Fyn complexes allowed the recruitment of COX-2 into the complex, leading to PGE_2 production (Fig. 8C). The third phase occurred when ACAT-1 was recruited into Aβ–PrP^C–$cPLA_2$–COX-2–Fyn complexes (Fig. 8D). The subsequent esterification of cholesterol reduced cholesterol concentrations, and led to the dispersal of complexes and the loss of $cPLA_2$, COX-2 and ACAT-1 from DRMs. These observations indicate that cholesterol esterification led to the dissociation of signalling complexes and reduced cell signalling.

In summary, the key finding of this study is that the Aβ-induced activation of CEH and increase in cholesterol concentrations in synaptosomes was dependent upon activated $cPLA_2$ and PAF. The increased cholesterol concentrations were associated with the migration of COX-2 and Fyn into lipid rafts and the production of PGE_2, a bioactive lipid that causes synapse degeneration at high concentrations. Crucially, this signalling pathway also facilitated the migration of ACAT-1 into the Aβ–PrP^C–$cPLA_2$–COX-2–Fyn complex. The subsequent cholesterol esterification reduced free cholesterol concentrations, resulting in the dissociation of this complex and the cessation of cell signalling.

MATERIALS AND METHODS

Primary neuronal cultures

Primary cortical neurons were prepared from the brains of mouse embryos (day 15.5) after mechanical dissociation. A total of 5×10^5 cells/well were dispensed in 48-well plates in Ham's F12 containing 5% fetal calf serum for 2 h. Cultures were shaken (600 rpm for 5 min), and non-adherent cells removed by two washes in phosphate-buffered saline (PBS). Neurons were grown in neurobasal medium containing B27 components and nerve growth factor (5 ng/ml) (Sigma-Aldrich) for 10 days. Immunostaining showed that, after 10 days culture, less than 5% of the viable cells stained for glial fibrillary acidic protein (GFAP) or F4/80 (astrocytes or microglial cells). Neurons were pre-treated with test compounds or vehicle controls for 1 h before the addition of test samples, including Aβ preparations or PLAP (Bachem), for 24 h. Stock solutions of these drugs were prepared in ethanol or dimethyl sulphoxide; vehicle controls consisted of equivalent dilutions of ethanol or dimethyl sulphoxide in neurobasal medium and B27 components. The culture medium was used as control medium (neurobasal medium containing B27 components). All experiments were performed in accordance with European regulations (European community Council Directive, 1986, 56/609/EEC) and were approved by the Royal Veterinary College ethical committee.

Isolation of synaptosomes

Synaptosomes were prepared on a discontinuous Percoll gradient, based on methods previously described (Thais et al., 2006). Briefly, 10^6 neurons were homogenised at 4°C in 1 ml of SED solution (0.32 M sucrose, 50 mM Tris-HCl pH 7.4, 1 mM EDTA and 1 mM dithiothreitol) and centrifuged (1000 ***g*** for 5 min). The supernatant was transferred to a four-step gradient of 3%, 10%, 15% and 23% Percoll in SED solution and centrifuged at 16,000 ***g*** for 30 min at 4°C. The synaptosomes were collected from the interface of the 15% and 23% Percoll steps and washed in PBS at 4°C. Freshly prepared synaptosomes were pre-treated with test compounds for 30 min and incubated with peptides for 1 h or the time stated. At the end of the experiment, synaptosomes were centrifuged at 16,000 ***g*** for 5 min at 4°C, and either total membrane extracts or DRMs were isolated as below.

To access the amounts of Aβ–PrP^C complexes at the surface of synaptosomes, synaptosomes were incubated with 0.5 ml phosphatidylinositol-specific phospholipase C (from *Bacillus cereus*, Sigma-Aldrich) for 10 min. This enzyme is cell impermeable and, consequently, only released PrP^C expressed on the surface of synaptosomes. Treated synaptosomes were centrifuged (16,000 ***g*** for 5 min), and the supernatant was collected and tested for Aβ–PrP^C complexes (see below).

Journal of Cell Science (2018) 131, jcs211789. doi:10.1242/jcs.211789

Total neuron and synaptosome extracts

Treated cells or synaptosomes were washed twice in PBS and homogenised in an extraction buffer containing 10 mM Tris-HCl, 100 mM NaCl, 10 mM EDTA, 0.5% Nonidet P-40, 0.5% sodium deoxycholate and 0.2% SDS at 10^6 cells/ml. Mixed protease inhibitors [4-(2-aminoethyl)benzenesulfonyl fluoride hydrochloride, aprotinin, leupeptin, bestatin, pepstatin A and E-46; Sigma-Aldrich] were added, and large insoluble fragments were removed by centrifugation (1000 ***g*** for 5 min).

Isolation of DRMs

DRMs were isolated by using their insolubility in non-ionic detergents, as described (London and Brown, 2000). Briefly, synaptosomes were homogenised in an ice-cold buffer containing 1% Triton X-100, 10 mM Tris-HCl, pH 7.2, 150 mM NaCl, 10 mM EDTA and mixed protease inhibitors (as above), and large fragments were removed by centrifugation (1000 ***g*** for 5 min at 4°C). The supernatant was incubated on ice (4°C) for 1 h and centrifuged (16,000 ***g*** for 30 min at 4°C). The supernatant (DSM) was collected. The insoluble pellet was homogenised in an extraction buffer containing 10 mM Tris-HCl, pH 7.4, 150 mM NaCl, 10 mM EDTA, 0.5% Nonidet P-40, 0.5% sodium deoxycholate, 0.2% SDS and mixed protease inhibitors, and centrifuged (10 min at 16,000 ***g***). The soluble material was reserved as the DRM fraction.

Co-precipitation studies

Synaptosomes were homogenised in an ice-cold buffer containing 1% Triton X-100 (as above), and large fragments were removed by centrifugation (1000 ***g*** for 5 min at 4°C). The supernatant was incubated with 1 µg/ml of the PrP^C-reactive mAb 4F2 or an isotype control for 1 h at 4°C, followed by the addition of 10 µl of protein G-coated beads (Sigma-Aldrich) for a further 10 min. The mixture was centrifuged at 1000 ***g*** for 5 min to collect beads and the attached PrP^C-containing DRMs. Beads were washed twice in ice-cold 1% Triton X-100 before use.

Western blotting

Samples were mixed with Laemmli buffer containing β-mercaptoethanol and heated to 95°C for 5 min; proteins were separated by electrophoresis on 15% polyacrylamide gels. Proteins were transferred onto a Hybond-P polyvinylidene membrane by semi-dry blotting and membranes blocked using 10% milk powder. Antibodies used are listed in Table S1. These were visualised using a combination of biotinylated anti-mouse/goat/rat/rabbit IgG (Sigma-Aldrich), extravidin–peroxidase and enhanced chemiluminescence.

Brain extracts

Soluble extracts from brain tissue (temporal lobes supplied by Asterand; informed consent was given to Asterand, and samples were collected according to the Declaration of Helsinki, 2000) of three patients with a clinical and pathologically-confirmed diagnosis of Alzheimer's disease were prepared, using methods as previously described (Shankar et al., 2008). Briefly, brain tissue was cut into approximately 100 mg pieces and added to 2 ml tubes containing lysing matrix D beads (Q-Bio). Tris-buffered saline (20 mM Tris-HCl, pH 7.4, 150 mM NaCl,) was added, so that there was the equivalent of 100 mg brain tissue/ml. Tubes were shaken for 10 min (Disruptor Genie, Scientific Industries) and centrifuged at 16,000 ***g*** for 10 min to remove cell debris. Soluble material was passed through a 50 kDa filter (Sartorius) to remove any protease activity, and desalted (3 kDa filter; Sartorius) to remove drugs and small molecules. The retained material contained peptides from 3-50 kDa and were stored at −80°C. For biological experiments, the soluble AD brain extracts were diluted in neurobasal medium containing B27 components. For immunoblot analysis, extracts were mixed with an equal volume of 0.5% NP-40, 5 mM CHAPS, 50 mM Tris-HCl, pH 7.4 and separated by polyacrylamide gel electrophoresis. Proteins were transferred onto a polyvinylidene membrane by semi-dry blotting and blocked using 10% milk powder. Aβ was detected by incubation with mAb 6E10 (reactive with an epitope 1-16 of Aβ; Covance, SIG 39340), biotinylated anti-mouse IgG, extravidin–peroxidase and enhanced chemiluminescence.

Immunodepletions

Soluble AD brain extracts were incubated with 1 µg/ml mAb 4G8 (reactive with epitope 17-24 of Aβ; Covance, SIG-39220) or 1 µg/ml mAb LN27 [reactive with epitope 45 to 53 of the amyloid precursor protein; Covance, SIG-39188 (mock-depletion)] and incubated at 4°C on rollers for 1 h. Protein G microbeads (Sigma-Aldrich) were added (10 µl/ml) for 30 min and protein G bound-antibody complexes removed by centrifugation at 16,000 ***g*** for 5 min. The treated AD brain extracts were filtered (0.2 µM; Sartorius) before use.

Synaptophysin ELISA

The amount of synaptophysin in neuronal extracts was measured by enzyme-linked immunosorbent assay (ELISA), as previously described (Bate et al., 2010). Maxisorb immunoplates (Nunc) were coated with 1 µg/ml of a mouse anti-synaptophysin mAb (MAB368; Millipore) as a capture antibody. Samples were applied (1 h at room temperature), and bound synaptophysin was detected using 1 µg/ml rabbit polyclonal anti-synaptophysin (Abcam, ab53166), followed by an anti-rabbit IgG conjugated to alkaline phosphatase (Sigma-Aldrich, A3687) and 1 mg/ml 4-nitrophenol phosphate solution (Sigma-Aldrich). Absorbance was measured on a microplate reader at 405 nm. Samples were expressed as 'units synaptophysin', where 100 units was defined as the amount of synaptophysin in 10^6 untreated neurons.

$cPLA_2$ ELISA and PGE_2 measurement

The amounts of $cPLA_2$ in extracts was measured by ELISA, as previously described (West et al., 2017). Maxisorb immunoplates were coated with 0.5 µg/ml of mouse mAb anti-$cPLA_2$ (clone CH-7; Upstate, 05-568) and blocked with 5% milk powder in PBS+0.1% Tween-20 (PBST). Samples were added for 1 h and the amount of bound $cPLA_2$ was detected using a goat polyclonal anti-$cPLA_2$ (Santa-Cruz Biotechnology, sc-4049), followed by biotinylated anti-goat IgG, extravidin–alkaline phosphatase and 1 mg/ml 4-nitrophenol phosphate solution. Absorbance was measured at 405 nm and the amount of $cPLA_2$ protein expressed in units; 100 units was defined as the amount of $cPLA_2$ in control preparations.

The concentrations of PGE_2 and PAF in synaptosomes were determined using competitive enzyme immunoassay kits (R&D Systems, Abingdon, UK), according to the manufacturer's instructions.

COX-1 ELISA

Maxisorb immunoplates were coated with 1 µg/ml mouse mAb to amino acids 575 to 602 of COX-1 (H-1, sc-166572, Santa Cruz Biotechnology) overnight and blocked with 5% milk powder. Samples were added for 1 h, and the amount of bound COX-1 was detected with 0.5 µg/ml of a rabbit polyclonal IgG to amino acids 63 to 124 of COX-1 (H-62, sc-7950, Santa Cruz Biotechnology), followed by a biotinylated anti-rabbit IgG (1:2000), extravidin–alkaline phosphatase and 1 mg/ml 4-nitrophenol phosphate solution. Absorbance was measured at 405 nm, and results were expressed as the percentage of COX-1, where 100% was defined as the amount of COX-1 in control synaptosomes.

COX-2 ELISA

Maxisorb immunoplates were coated with 1 µg/ml mouse mAb (5E10/D10; Enzo Life Sciences) overnight and blocked with 5% milk powder. Samples were added for 1 h, and the amount of bound COX-2 was detected with 0.5 µg/ml of rabbit polyclonal IgG to epitope 50 to 111 (H-62; Santa Cruz, sc-7951), followed by a biotinylated rabbit anti-goat IgG (Sigma, 1:2000), extravidin–alkaline phosphatase and 1 mg/ml 4-nitrophenol phosphate solution. Absorbance was measured at 405 nm, and results were expressed as the percentage of COX-2, where 100% was defined as the amount of COX-2 in control synaptosomes.

ACAT-1 ELISA

Maxisorb immunoplates were coated with 1 µg/ml rabbit monoclonal anti-ACAT-1 (EPR10359; ab168342, Abcam, 1:1000) overnight and blocked with 5% milk powder in PBS+2% Tween-20. Samples were added for 1 h, and the amount of bound ACAT-1 was detected with 0.5 µg/ml of a goat polyclonal IgG (G-15; sc-161307, Santa Cruz Biotechnology), followed

by a biotinylated rabbit anti-goat IgG (1:2000), extravidin–alkaline phosphatase and 1 mg/ml 4-nitrophenol phosphate solution. Absorbance was measured at 405 nm, and results were expressed as the percentage of ACAT-1, where 100% was defined as the amount of ACAT-1 in control synaptosomes.

Aβ–PrP^C complex ELISA

The amounts of Aβ–PrP^C complexes in synaptosomes was measured by ELISA, as previously described (West et al., 2017). Maxisorb immunoplates were coated with mAb 4F2 reactive with PrP^C. Plates were blocked with 5% milk powder, and samples were added for 1 h. Aβ bound to PrP^C was detected by using biotinylated mAb 6E10 (Covance). Bound Aβ was detected using extravidin–alkaline phosphatase and 1 mg/ml 4-nitrophenol phosphate solution, and absorbance was measured at 405 nm. Samples were expressed as a percentage of maximum optical density in control synaptosomes.

Preparation of samples for $A\beta_{42}$ ELISA

To detach $A\beta_{42}$ from membrane components that blocked specific epitopes, samples (300 µl) were mixed with 700 µl of propan-2-ol and sonicated. Proteins were precipitated by addition of 250 µl 100% w/v trichloroacetic acid, incubation on ice for 30 min and centrifugation (16,000 ***g*** for 10 min at 4°C). The pellet was washed twice with ice-cold acetone, dried, suspended in a buffer containing 150 mM NaCl, 10 mM Tris-HCl, pH 7.4, 10 mM EDTA and 0.2% SDS, and sonicated.

$A\beta_{42}$ ELISA

Nunc Maxisorb immunoplates were coated with mAb 4G8 in carbonate buffer overnight. Plates were blocked with 5% milk powder in PBST, and samples were applied. The detection antibody was an $A\beta_{42}$-selective rabbit mAb BA3-9 (Covance, SIG-39168), followed by biotinylated anti-rabbit IgG and extravidin–alkaline phosphatase. Total Aβ was visualised by addition of 1 mg/ml p-nitrophenol phosphate solution, and optical density at 405 nm was measured in a spectrophotometer.

Cholesterol content

The concentrations of cholesterol in samples were measured using the Amplex Red cholesterol assay kit (Life Technologies, Paisley, UK) (Robinet et al., 2010), according to the manufacturer's instructions. Briefly, cholesterol was oxidised by cholesterol oxidase to yield hydrogen peroxide and ketones. The hydrogen peroxide reacted with 10-acetyl-3,7-dihydroxyphenoxazine (Amplex Red reagent) to produce highly fluorescent resorufin, which was measured by excitation at 550 nm and emission detection at 590 nm. By performing the assay in the presence or absence of cholesterol esterase, we were also able to determine the amounts of esterified cholesterol within samples. Each experiment contained cholesterol standards and solvent-only controls. Cholesterol concentrations were calculated by reference to the cholesterol standards.

Statistical methods

Differences between treatment groups were assessed using paired Student's *t*-tests, and one-way and two-way ANOVA with Bonferroni's post hoc tests (IBM SPSS statistics 20). Error values are ±s.d. Correlations were determined using bivariate analysis, and significance was set at 0.01%.

Acknowledgements

We would like to thank Professor Alun Williams (Cambridge University, UK) for supplying human brain material.

Competing interests

The authors declare no competing or financial interests.

Author contributions

Conceptualization: C.O., E.W., C.B.; Methodology: C.O., E.W., C.B.; Formal analysis: C.B.; Investigation: C.O., E.W., C.B.; Data curation: C.O., E.W., C.B.; Writing - original draft: C.B.; Writing - review & editing: C.B.; Supervision: C.B.; Project administration: C.B.

Funding

This work was funded by the Royal Veterinary College Bioveterinary Sciences undergraduate project funds.

Supplementary information

Supplementary information available online at
http://jcs.biologists.org/lookup/doi/10.1242/jcs.211789.supplemental

References

Abramov, E., Dolev, I., Fogel, H., Ciccotosto, G. D., Ruff, E. and Slutsky, I. (2009). Amyloid-[beta] as a positive endogenous regulator of release probability at hippocampal synapses. *Nat. Neurosci.* **12**, 1567-1576.

Bate, C. and Williams, A. (2011). Amyloid-β-induced synapse damage is mediated via cross-linkage of the cellular prion protein. *J. Biol. Chem.* **286**, 37955-37963.

Bate, C., Tayebi, M. and Williams, A. (2010). Phospholipase A_2 inhibitors protect against prion and Aβ mediated synapse degeneration. *Mol. Neurodegener.* **5**, 13.

Bhattacharyya, D. K., Lecomte, M., Dunn, J., Morgans, D. J. and Smith, W. L. (1995). Selective inhibition of prostaglandin endoperoxide synthase-1 (Cyclooxygenase-1) by valerylsalicylic acid. *Arch. Biochem. Biophys.* **317**, 19-24.

Brown, D. A. and London, E. (2000). Structure and function of sphingolipid- and cholesterol-rich membrane rafts. *J. Biol. Chem.* **275**, 17221-17224.

Bryleva, E. Y., Rogers, M. A., Chang, C. C. Y., Buen, F., Harris, B. T., Rousselet, E., Seidah, N. G., Oddo, S., LaFerla, F. M., Spencer, T. A. et al. (2010). ACAT1 gene ablation increases 24(S)-hydroxycholesterol content in the brain and ameliorates amyloid pathology in mice with AD. *Proc. Natl. Acad. Sci. USA* **107**, 3081-3086.

Caetano, F. A., Lopes, M. H., Hajj, G. N. M., Machado, C. F., Pinto Arantes, C., Magalhaes, A. C., Vieira, M. D. P. B., Americo, T. A., Massensini, A. R., Priola, S. A. et al. (2008). Endocytosis of prion protein is required for ERK1/2 signaling induced by stress-inducible protein 1. *J. Neurosci.* **28**, 6691-6702.

Chang, T.-Y., Chang, C. C. Y., Ohgami, N. and Yamauchi, Y. (2006). Cholesterol sensing, trafficking, and esterification. *Annu. Rev. Cell Dev. Biol.* **22**, 129-157.

Chen, C. and Bazan, N. G. (2005). Endogenous PGE_2 regulates membrane excitability and synaptic transmission in hippocampal CA1 pyramidal neurons. *J. Neurphysiol.* **93**, 929-941.

Chen, C., Magee, J. C., Marcheselli, V., Hardy, M. and Bazan, N. G. (2001). Attenuated LTP in hippocampal dentate gyrus neurons of mice deficient in the PAF receptor. *J. Neurophysiol.* **85**, 384-390.

Chiesa, R., Piccardo, P., Biasini, E., Ghetti, B. and Harris, D. A. (2008). Aggregated, wild-type prion protein causes neurological dysfunction and synaptic abnormalities. *J. Neurosci.* **28**, 13258-13267.

Clark, G. D., Happel, L. T., Zorumski, C. F. and Bazan, N. G. (1992). Enhancement of hippocampal excitatory synaptic transmission by platelet-activating factor. *Neuron* **9**, 1211-1216.

Copeland, R. A., Williams, J. M., Giannaras, J., Nurnberg, S., Covington, M., Pinto, D., Pick, S. and Trzaskos, J. M. (1994). Mechanism of selective inhibition of the inducible isoform of prostaglandin G/H synthase. *Proc. Natl. Acad. Sci. USA* **91**, 11202-11206.

Garcia-Osta, A. and Alberini, C. M. (2009). Amyloid beta mediates memory formation. *Learn. Mem.* **16**, 267-272.

Gylys, K. H., Fein, J. A., Yang, F., Miller, C. A. and Cole, G. M. (2007). Increased cholesterol in A[beta]-positive nerve terminals from Alzheimer's disease cortex. *Neurobiol. Aging* **28**, 8-17.

Haass, C., Schlossmacher, M. G., Hung, A. Y., Vigo-Pelfrey, C., Mellon, A., Ostaszewski, B. L., Lieberburg, I., Koo, E. H., Schenk, D. and Teplow, D. B. (1992). Amyloid β-peptide is produced by cultured cells during normal metabolism. *Nature* **359**, 322-325.

Herms, J., Tings, T., Gall, S., Madlung, A., Giese, A., Siebert, H., Schurmann, P., Windl, O., Brose, N. and Kretzschmar, H. (1999). Evidence of presynaptic location and function of the prion protein. *J. Neurosci.* **19**, 8866-8875.

Kato, K., Clark, G. D., Bazan, N. G. and Zorumski, C. F. (1994). Platelet-activating factor as a potential retrograde messenger in CA1 hippocampal long-term potentiation. *Nature* **367**, 175-179.

Kaufmann, W. E., Worley, P. F., Pegg, J., Bremer, M. and Isakson, P. (1996). COX-2, a synaptically induced enzyme, is expressed by excitatory neurons at postsynaptic sites in rat cerebral cortex. *Proc. Natl. Acad. Sci. USA* **93**, 2317-2321.

Koch, H., Huh, S.-E., Elsen, F. P., Carroll, M. S., Hodge, R. D., Bedogni, F., Turner, M. S., Hevner, R. F. and Ramirez, J.-M. (2010). Prostaglandin E2-induced synaptic plasticity in neocortical networks of organotypic slice cultures. *J. Neurosci.* **30**, 11678-11687.

Kotilinek, L. A., Westerman, M. A., Wang, Q., Panizzon, K., Lim, G. P., Simonyi, A., Lesne, S., Falinska, A., Younkin, L. H., Younkin, S. G. et al. (2008). Cyclooxygenase-2 inhibition improves amyloid-beta-mediated suppression of memory and synaptic plasticity. *Brain* **131**, 651-664.

Lacor, P. N., Buniel, M. C., Chang, L., Fernandez, S. J., Gong, Y., Viola, K. L., Lambert, M. P., Velasco, P. T., Bigio, E. H., Finch, C. E. et al. (2004). Synaptic targeting by Alzheimer's-related amyloid β oligomers. *J. Neurosci.* **24**, 10191-10200.

Laurén, J., Gimbel, D. A., Nygaard, H. B., Gilbert, J. W. and Strittmatter, S. M. (2009). Cellular prion protein mediates impairment of synaptic plasticity by amyloid-β oligomers. *Nature* **457**, 1128-1132.
Linden, R., Cordeiro, Y. and Lima, L. M. T. R. (2012). Allosteric function and dysfunction of the prion protein. *Cell. Mol. Life Sci.* **69**, 1105-1124.
London, E. and Brown, D. A. (2000). Insolubility of lipids in Triton X-100: physical origin and relationship to sphingolipid/cholesterol membrane domains (rafts). *Biochim. Biophys. Acta* **1508**, 182-195.
Millman, E. E., Zhang, H., Godines, V., Bean, A. J., Knoll, B. J. and Moore, R. H. (2008). Rapid recycling of beta-adrenergic receptors is dependent on the actin cytoskeleton and myosin Vb. *Traffic* **9**, 1958-1971.
Montine, T. J., Sidell, K. R., Crews, B. C., Markesbery, W. R., Marnett, L. J., Roberts, L. J. and Morrow, J. D. (1999). Elevated CSF prostaglandin E2 levels in patients with probable AD. *Neurology* **53**, 1495-1498.
Mouillet-Richard, S., Ermonval, M., Chebassier, C., Laplanche, J. L., Lehmann, S., Launay, J. M. and Kellermann, O. (2000). Signal transduction through prion protein. *Science* **289**, 1925-1928.
Palavicini, J. P., Wang, C., Chen, L., Hosang, K., Wang, J., Tomiyama, T., Mori, H. and Han, X. (2017). Oligomeric amyloid-beta induces MAPK-mediated activation of brain cytosolic and calcium-independent phospholipase A2 in a spatial-specific manner. *Acta Neuropathol. Commun.* **5**, 56.
Puglielli, L., Konopka, G., Pack-Chung, E., Ingano, L. A. M. K., Berezovska, O., Hyman, B. T., Chang, T. Y., Tanzi, R. E. and Kovacs, D. M. (2001). Acyl-coenzyme A: cholesterol acyltransferase modulates the generation of the amyloid beta-peptide. *Nat. Cell Biol.* **3**, 905-912.
Puzzo, D., Privitera, L., Fa, M., Staniszewski, A., Hashimoto, G., Aziz, F., Sakurai, M., Ribe, E. M., Troy, C. M., Mercken, M. et al. (2011). Endogenous amyloid-β is necessary for hippocampal synaptic plasticity and memory. *Ann. Neurol.* **69**, 819-830.
Rajendran, L. and Simons, K. (2005). Lipid rafts and membrane dynamics. *J. Cell Sci.* **118**, 1099-1102.
Riendeau, D., Percival, M. D., Boyce, S., Brideau, C., Charleson, S., Cromlish, W., Ethier, D., Evans, J., Falgueyret, J.-P., Ford-Hutchinson, A. W. et al. (1997). Biochemical and pharmacological profile of a tetrasubstituted furanone as a highly selective COX-2 inhibitor. *Br. J. Pharmacol.* **121**, 105-117.
Robinet, P., Wang, Z., Hazen, S. L. and Smith, J. D. (2010). A simple and sensitive enzymatic method for cholesterol quantification in macrophages and foam cells. *J. Lipid Res.* **51**, 3364-3369.
Ryan, S. D., Whitehead, S. N., Swayne, L. A., Moffat, T. C., Hou, W., Ethier, M., Bourgeois, A. J. G., Rashidian, J., Blanchard, A. P., Fraser, P. E. et al. (2009). Amyloid-β42 signals tau hyperphosphorylation and compromises neuronal viability by disrupting alkylacylglycerophosphocholine metabolism. *Proc. Natl. Acad. Sci. USA* **106**, 20936-20941.
Sang, N., Zhang, J., Marcheselli, V., Bazan, N. G. and Chen, C. (2005). Postsynaptically synthesized prostaglandin E2 (PGE2) modulates hippocampal synaptic transmission via a presynaptic PGE2 EP2 receptor. *J. Neurosci.* **25**, 9858-9870.
Selkoe, D. J. (2002). Alzheimer's disease is a synaptic failure. *Science* **298**, 789-791.
Shankar, G. M., Li, S., Mehta, T. H., Garcia-Munoz, A., Shepardson, N. E., Smith, I., Brett, F. M., Farrell, M. A., Rowan, M. J., Lemere, C. A. et al. (2008). Amyloid-β protein dimers isolated directly from Alzheimer's brains impair synaptic plasticity and memory. *Nat. Med.* **14**, 837-842.
Smith, C. J., Zhang, Y., Koboldt, C. M., Muhammad, J., Zweifel, B. S., Shaffer, A., Talley, J. J., Masferrer, J. L., Seibert, K. and Isakson, P. C. (1998). Pharmacological analysis of cyclooxygenase-1 in inflammation. *Proc. Natl Acad. Sci. USA* **95**, 13313-13318.
Solforosi, L., Criado, J. R., McGavern, D. B., Wirz, S., Sanchez-Alavez, M., Sugama, S., DeGiorgio, L. A., Volpe, B. T., Wiseman, E., Abalos, G. et al. (2004). Cross-linking cellular prion protein triggers neuronal apoptosis in vivo. *Science* **303**, 1514-1516.
Takahashi, R. H., Capetillo-Zarate, E., Lin, M. T., Milner, T. A. and Gouras, G. K. (2010). Co-occurrence of Alzheimer's disease beta-amyloid and tau pathologies at synapses. *Neurobiol. Aging* **31**, 1145-1152.
Taraboulos, A., Scott, M., Semenov, A., Avrahami, D., Laszlo, L., Prusiner, S. B. and Avraham, D. (1995). Cholesterol depletion and modification of COOH-terminal targeting sequence of the prion protein inhibit formation of the scrapie isoform. *J. Cell Biol.* **129**, 121-132.
Thais, M. E., Carqueja, C. L., Santos, T. G., Silva, R. V., Stroeh, E., Machado, R. S., Wahlheim, D. O., Bianchin, M. M., Sakamoto, A. C., Brentani, R. R. et al. (2006). Synaptosomal glutamate release and uptake in mice lacking the cellular prion protein. *Brain Res.* **1075**, 13-19.
West, E., Osborne, C. and Bate, C. (2017). The cholesterol ester cycle regulates signalling complexes and synapse damage caused by amyloid-β. *J. Cell Sci.* **130**, 3050-3059.
Xu, X., Bittman, R., Duportail, G., Heissler, D., Vilcheze, C. and London, E. (2001). Effect of the structure of natural sterols and sphingolipids on the formation of ordered sphingolipid/sterol domains (rafts). Comparison of cholesterol to plant, fungal, and disease-associated sterols and comparison of sphingomyelin, cerebrosides, and ceramide. *J. Biol. Chem.* **276**, 33540-33546.
Yang, T., Li, S., Xu, H., Walsh, D. M. and Selkoe, D. J. (2017). Large soluble oligomers of amyloid β-protein from Alzheimer brain are far less neuroactive than the smaller oligomers to which they dissociate. *J. Neurosci.* **37**, 152-163.
Zhu, D., Lai, Y., Shelat, P. B., Hu, C., Sun, G. Y. and Lee, J. C.-M. (2006). Phospholipases A_2 mediate amyloid-β peptide-induced mitochondrial dysfunction. *J. Neurosci.* **26**, 11111-11119.